QZFM Crosstalk

Michael Zhao

March 2024

1 Introduction

The Quspin Zero Field Magnetometer (QZFM) is intended to be used for mapping the magnetic environment to high precision and accuracy for the nEDM experiment at TRIUMF. The group possesses 2 third-generation QZFMs, which makes possible the possibility of operating both sensors simultaneously. One potential benefit of reading two sensors simultaneously is the extraction of gradient information. However, when sensors are operated in close proximity to one another, crosstalk effects tend to arise and must be carefully understood for the magnetic field reading to remain trustworthy.

2 Sources of Crosstalk

The QZFM has two main sources of crosstalk, both stemming from fundamental principles of rubidium-based magnetometers. For quantum mechanical reasons, rubidium atoms become transparent to light when the background magnetic field is near zero, and by measuring the output of a photo-detector, one sees the response follows a Lorentzian shape as a function of magnetic field, and the magnetic field is the deviation from the peak of the Lorentzian. A direct measurement of the deviation is sensitive to pink noise (1/f), but this can be alleviated if one introduces a high-frequency amplitude modulation and monitors the modulation field instead. [4] To this end, the QZFM contains an internal coil that drives a modulation field at 923 Hz with an amplitude of 60 nT. [4, 2] The electronic module contains a phase-sensitive lock-in detector and demodulates the photo-detector output from the 923 Hz signal to obtain the analog output. Since the modulation field is internally generated using a set of coils, the first source of crosstalk appears when the modulation fields of two separate sensors in proximity interfere with each other. This issue is mitigated to an extent through the designation of 'master' and 'slave' sensors, whereby the master sensor provides the same modulation signal relayed to all the slaves, which solves any phase lag between sensors and avoids signals adding constructively or destructively. However, one problem remains in that the fields will still superimpose on each other. Crucially, the sensitive direction of each sensor is determined by the direction of the modulation field. Therefore, the sensitive axis of the two sensors can be changed if they are placed in close proximity. Furthermore, the effective magnitude of the modulation field is also likely changed. This effect is explored theoretically in a publication by Tiernal et al. [4].

The second source of crosstalk stems from the zero-field requirement of QZFMs. Since even in most multi-layered magnetically shielded rooms (MSRs) the residual field is on the order of several tens of nano-teslas, each QZFM comes equipped with its own tri-axial Helmholtz coil around the rubidium cell, which can null up to 50 nT of residual field. This becomes a problem when two sensors are in proximity, and the compensation coil of one sensor can 'knock' the nearby sensors out of zero-field. To address this problem, the best solution seems to be to zero both sensors simultaneously and let the two independent PID algorithms find the most optimal way to null the field at the two locations as well as it can. This report will be focused on the first source of crosstalk.

In this study, we try to answer the question: '**What is the minimal distance at which the crosstalk effects between two sensors are negligible?**' Two experiments were performed to answer this question.

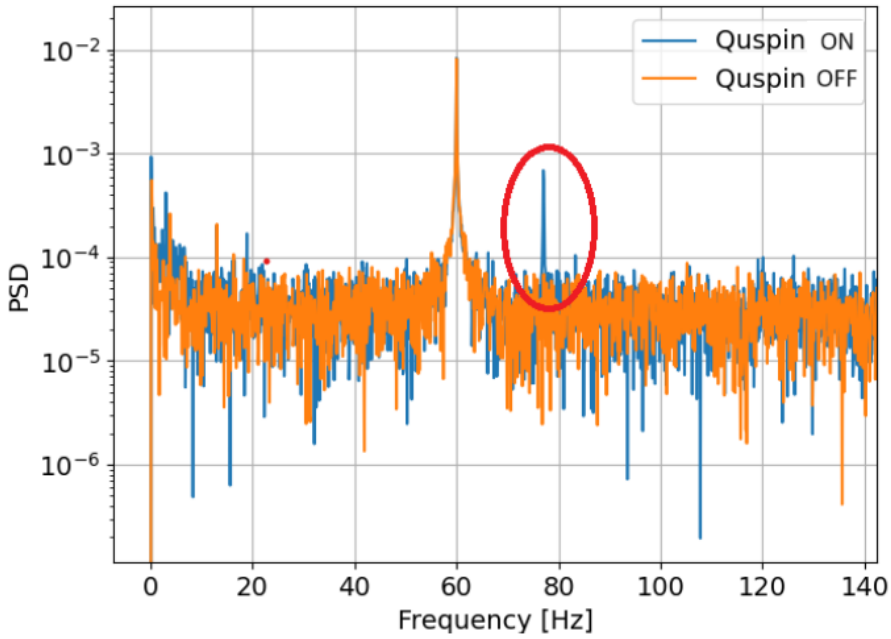

Figure 1: Two power spectrum densities from time series measured using the Stefan Mayer Fluxgate placed 1.5 cm from the QZFM cell. When the QZFM is powered on, a 77 Hz peak (red circle) appears, which is exactly the frequency of the modulation field after aliasing effects.

3 Experiment I: Crosstalk Effect Measured Using a None-QZFM sensor

3.1 Methods and Apparatus

Since the crosstalk originates from the presence of the 923 Hz modulation field 'leaking' out of the Helmholtz coil into external space, we use a non-QZFM magnetometer to monitor this presence as a function of time. From a practical perspective, the 923 Hz will show up in a different frequency bin from aliasing effects, depending on the sampling frequency. Here we choose a sampling rate of 1000 Hz, and thus the modulation frequency will appear to have a frequency equal to $1000 - 923 = 77$ Hz. Note that the reason why we cannot simply use a second QZFM to monitor this frequency component is because the other QZFM contains its own modulation field at the exact same frequency, therefore it will always measure a mix between its own and the true external perturbing field. For the None-QZFM sensor, a Stefan Mayer Fluxmaster fluxgate magnetometer is chosen, for its compact size and relatively low intrinsic noise. These two properties will allow us the greatest flexibility in the measurable distance. In Fig. 1 two periodograms are overlaid, both measured from the fluxgate, placed 1.5 cm away from the QZFM rubidium cell. The difference in the spectrum density is clearly the additional presence of a 77 Hz spike after the QZFM has been switched on.

The baseline distance between the fluxgate and the cell is varied, from 0.5 cm (touching) to up to 7.5 cm in 1 cm intervals. 5 segments of 10 seconds each are recorded for each baseline distance. The 77 Hz is isolated by first passing the raw time series through a 2 Hz bandwidth band-pass filter centered on 77 Hz, and then the amplitude is measured using curve-fitting. The white intrinsic noise will have some component in the frequency pass band and will influence the measured amplitude. To compensate for this, an estimate for the intrinsic noise is gathered by performing the same analysis on segments of data where the QZFM is powered off. This noise contribution is then subsequently subtracted from all measured amplitude when the QZFM is powered on.

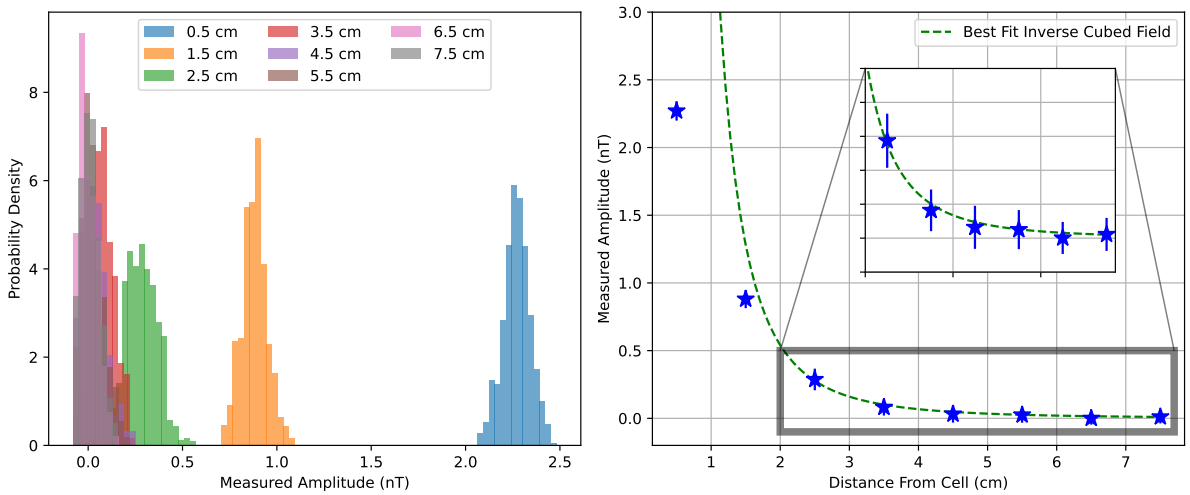

Figure 2: Left: Histogram of the measured amplitude of the 923 Hz (aliased to 77 Hz) modulation field using a fluxgate at each distance. Right: Measured amplitude vs. distance. The Green dotted line is fitted inverse cube function $\sim 1/r^3$. This is the functional form of a magnetic dipole, which is the far-field approximation for circular coils.

3.2 Results

The results are shown in Fig. 2. On the left, the histogram of the measured amplitude at each distance is shown. On the right, the measured amplitude as a function of baseline distance is plotted. Aside from the obvious decreasing behavior of the amplitude as the distance gets larger, we also expect for distances $r >> a$, where a is the radius of the coil generating the modulation field, the functional form of the decrease to be $\sim 1/r^3$, that of a magnetic dipole, which is the far-field approximation for coils. The fit is good for distances larger than about 1.5 cm. Introducing one commonly used metric to quantify crosstalk as a percentage:

$$\mathrm{CT}(r) = \frac{\text{Mod Amplitude at Distance } r}{\text{Mod Amplitude at Center of Cell}} \tag{1}$$

Using this definition, even directly outside the cell at 0.5 cm the crosstalk is already less than 5 percent, and above 6 cm it is essentially negligible. (At the center of the coil, the field strength is 60 nT, according to [4]) The results are consistent with other studies in the past that reported less than 3 percent crosstalk at 2 cm baseline [1].

4 Experiment II: Crosstalk Effect Measured Using a QZFM

4.1 Methods and Apparatus

In the second experiment, we measure the crosstalk effects of a QZFM on a second QZFM directly. Two QZFM gen 3 sensors are installed onto two rail carts whose distance can be linearly varied on an aluminum extrusion beam, shown in fig. 3.

The TUCAN group has two QZFM gen 3 in its inventory, of serial numbers AAL9 and AAY4. For this study, sensor number AAL9 remains fixed in place and acts as the primary sensor, from which all magnetic readings will be taken. Sensor number AAY4 serves as the perturbing sensor, and its distance to the primary sensor AAL9 will be shifted in one-centimeter intervals, starting from the minimum possible distance where the two sensor housings are directly touching. A single-turn coil of radius 170 mm is roughly centered on the primary sensor AAL9. The coil is connected to an external arbitrary waveform generator (AWG) of model

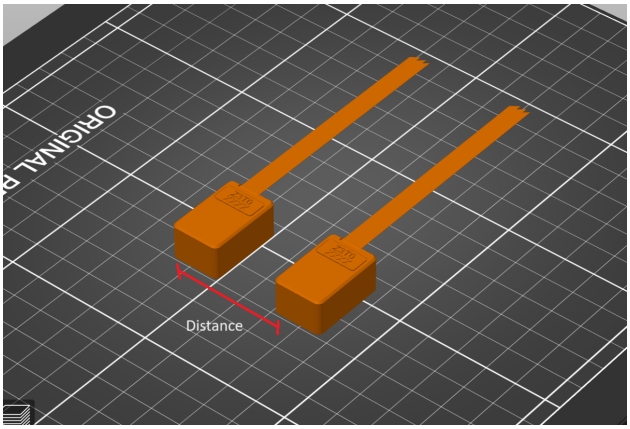

(a) Computer model of two QZFMs, showing how their distance is to be varied.

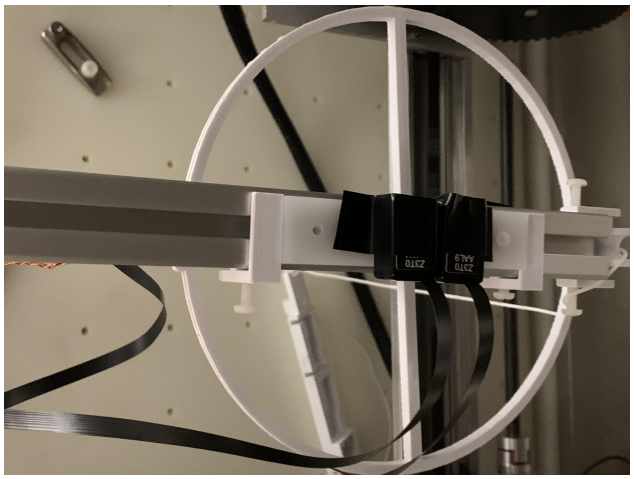

(b) Photo of setup. A background coil (white) generates an excitation field, and the two sensors are installed on slide-able trays. The entire setup is inside of a two-layer magnetic shielded room.

Figure 3: Experimental Setup

number Rigol DG1032Z, and a 35 Hz sinusoidal voltage is driven across the coil. This serves as the excitation signal used to quantify the gain change that results from the shift in the sensitive axis of the QZFM. The overall experiment is done three times, each time the excitation coil is realigned with one of the three sensor axes.

The measurement procedure is as follows:

1. The primary sensor is field zeroed.
2. The AWG turns on and drives the 35 Hz excitation voltage across the coil.
3. The primary sensor measures for 10 seconds.
4. Repeat steps 3 several times (e.g., 5 times), for increased statistical significance. The reason why individual segments are chosen over a continuous long measurement is to have the freedom to reject segments that may contain artifacts that would distort the result.
5. Power on the perturbing sensor.
6. Perform Steps 1-4.

From the recorded data, we wish to extract the amplitude of the excitation signal. The signal contains various other components - intrinsic noise, power-line interference, etc. All these will have a considerable influence on the analysis. Therefore, the signal is first passed through a 3rd order digital Butterworth band-pass filter implemented in Python, with the passing bandwidth between 34 and 36 Hz. The output time series will initially experience some large overshoots due to Gibbs' phenomenon. This is carefully truncated before the next step of analysis.

Now the amplitude from the cleaned time series is extracted via polynomial curve fitting on each individual crest and trough of the oscillation. The amplitude measured for a particular baseline between the two sets is compared for the two cases when the perturbing sensor is powered off, and when it has been switched on. To illustrate the effect of this shift, consider Fig. 4. Two measurements are taken in immediate succession, in the first only the primary sensor AAL9 is powered on, and in the second the perturbing sensor AAY4 is powered on also. The two sensors here are directly adjacent to each other, or about 1 cm apart. All the while the AWG drives the 35 Hz excitation signal through the coil. Recall that all field readings come from the primary sensor. On the left graph is shown a scatter plot of the fitted peak-to-peak amplitude of the excitation 35 Hz signal, blue stars represent those measured with only the primary sensor powered on, and the orange those measured after the powering of the perturbing sensor. A very obvious shift can be discerned. In the right figure, the same sets of amplitudes are shown as histograms. The statistical significance is even more apparent in this perspective. It should be noted that the histogram is not strictly Gaussian, as is obvious that there seems to be an extruding 'tail' on the low end of the range. In fact, this is but a symptom of a wider problem: it was seen that the distributions tend to stay very similar before and after switching on the perturbing sensor, but their distribution is often non-Gaussian, sometimes composed of several peaks. See fig. 5 for one such example. The cause of this is not pinpointed but could be potentially caused by small inconsistencies of the AWG for instance, or from temperature fluctuations of the rubidium cell.

Some attention will now be diverted to the question of how to determine the distance at which cross-talk ceases to be a prominent effect. Visually, if one compares the histograms such as in Fig. 4, but for successively longer baselines, the shifts will start to shrink until it is no longer discernible. One could look at the amount of shift in terms of the difference in the mean value of amplitude, in the unit of magnetic field density, but this is not a good metric since the absolute value of the shift is dependent on the strength of the background field (ie., if the background field is large, then a small change in the sensitive axis will result in a relatively big difference in the measured field). It is therefore useful to somehow normalize the shift, thus developing a more universal standard of comparison. Because the distributions are often non-normal, it is not very meaningful to divide the shift with the standard deviation. Instead, the following metric is chosen: For a particular sensing direction, all the shifts are divided by the shift magnitude when the two sensors are

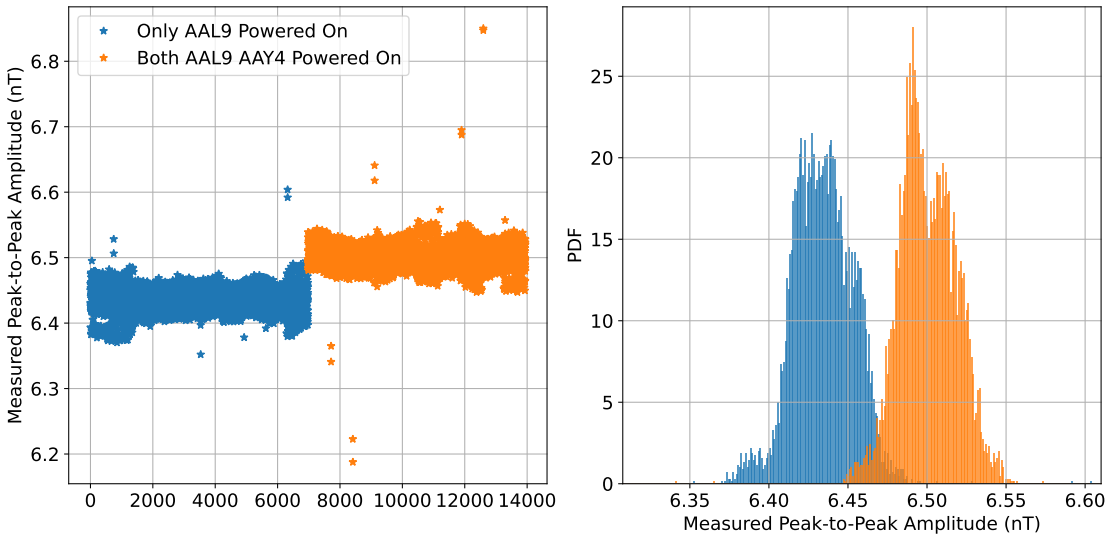

Figure 4: Example of the effect of modulation on the sensitive axis. When a second QZFM is switched on, the leaking modulation field superimposes on the other QZFM, altering the effective direction of the field, and thereby the sensitive axis of the sensor. This effect can be seen very clearly here, as when the second perturbing sensor is started the magnetic field measured suddenly shifts by a highly statistically significant amount.

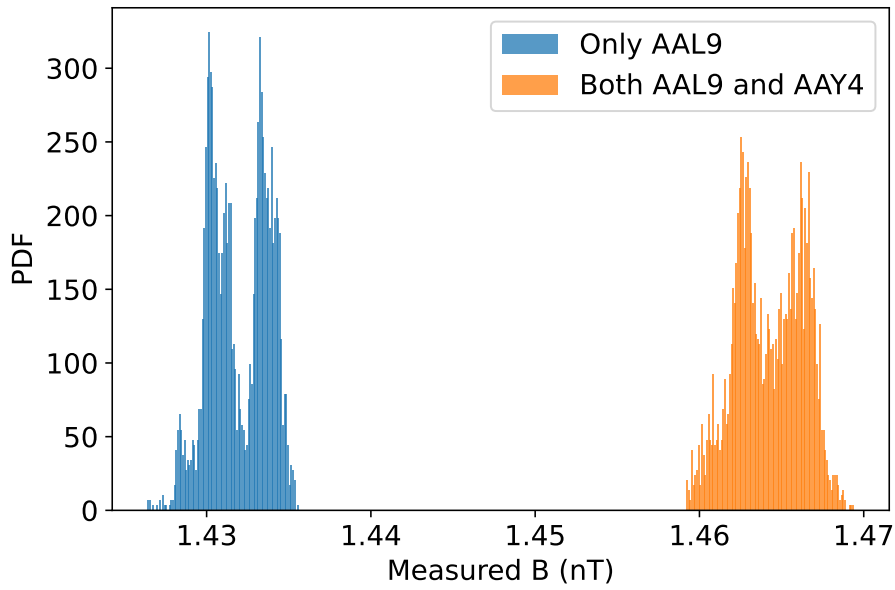

Figure 5: An example of a highly non-normal distribution in the observed amplitude.

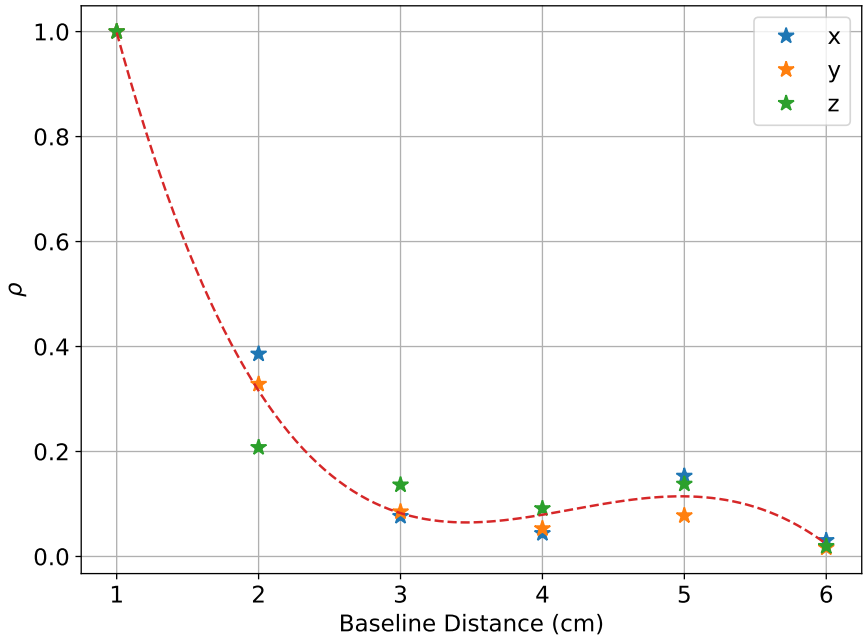

Figure 6: Crosstalk effect ρ as defined in Eq. 2 as a function of baseline distance. ρ can be interpreted as a percentage of amplitude shift as referenced to the amplitude shift when two sensors are directly adjacent. A small unexplained bump is observed at 5 cm in an otherwise monotonously decreasing trend.

directly touching. Denote this metric as ρ, we have

$$\rho(b) = \frac{s(b)}{s_0} \tag{2}$$

where b is the baseline distance, $s(b)$ is the shift in magnetic field amplitude at distance b, and s_0 is the shift when the two sensors are touching. The interpretation for ρ is the percentage of amplitude shift as referenced to the amplitude shift when two sensors are directly adjacent. **Keep in mind this is emphatically not the same as the concept of crosstalk percent defined in Eq. 1**

4.2 Results

The main results are shown in Fig. 6. $\rho(b)$ as defined in 2 is calculated starting with the two sensors directly touching (roughly 1 cm) and then in 1 cm intervals until 6 cm. The cross-talk defined in this sense sees a very rapid drop-off with baseline distance, already losing about 90 percent at 3 cm, though interestingly for all three directions (which recall is measured in 3 independent campaigns) a small rebound is observed at 5 cm baseline. At 6 cm, the crosstalk is less than 5 percent as referenced to the initial amount in all three directions.

5 Conclusion

In this report, we addressed the question of crosstalk among two QZFM sensors placed in close proximity. The root cause of the crosstalk is traced back to the mutual interference of the modulation field, which is generated from internal coils and will therefore suffer some amount of leakage into the external space. Two experiments were performed to quantify this effect, the first utilizes an external fluxgate sensor to measure

the leakage field strength as a function of distance. It was found that the leak is small, already only 5 percent of the field amplitude can be detected at the outer cell housing, and the effect is almost completely negligible beyond 6 cm. In the second experiment, a second QZFM is used to understand the gain change resulting from a shift in the sensitive axis created by the superposition of the modulation field from itself and the perturbing sensor. In this case, it was also found that beyond 6 cm very little crosstalk effects remain. Therefore, this study recommends for safe operations a minimal baseline of 6 cm should be allowed between the two sensors.

A Multi-sensor Operation

For completeness, we return to the second source of crosstalk mentioned in section 2, where the offset compensation fields of the two sensors may knock each other out of the zero field regime. Here a brief demonstration is given that as long as simultaneous zeroing is done, this does not hinder sensor operations. **The two sensors are placed with a baseline of 7 cm**. As a preliminary step, ensure the two sensors are operated in a master-slave configuration. This has to be done using the Quspin UI, which can be downloaded on their webpage [3]. To set a sensor as master, send command 113, and to set a sensor as slave, send command 114 in the terminal provided. Next, connect the modulation cables in the back of the electronics module from the master sensor to the mod in plug on the slave sensor. These two steps are shown in Fig. 7 and 8. If additional sensors are present, simply repeat this by connecting mod out of slave 1 to mod in of slave 2, and so on.

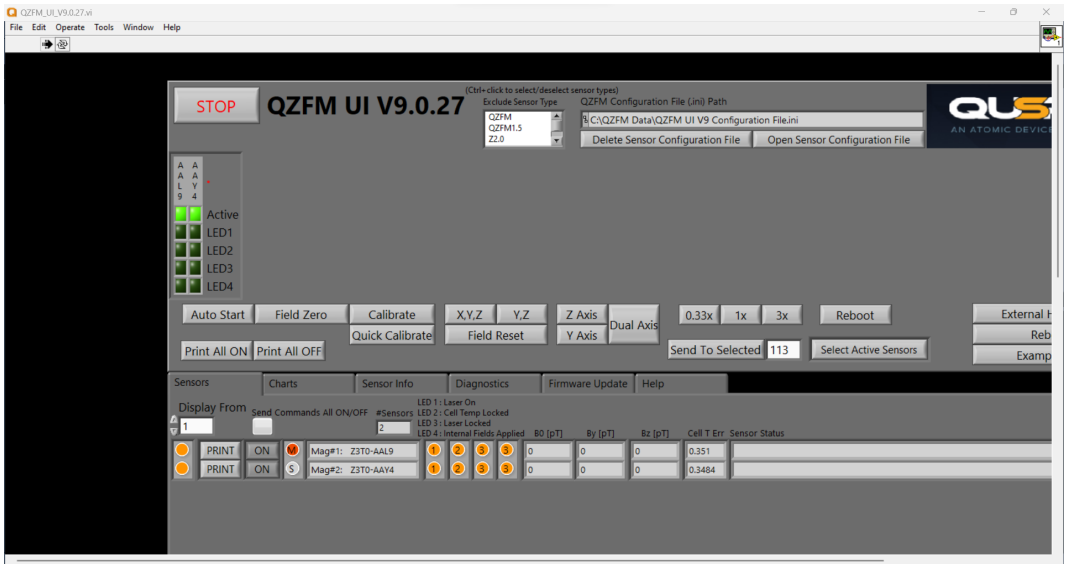

Figure 7: Screenshot of Quspin UI. Here sensor AAL9 is set as master and AAY4 is set as slave. To change status, send commands 113 and 114 for master/slave respectively.

As it is necessary to simultaneously zero the two sensors, a script based on multi-threading is developed in Python. The two sensors were given 60 seconds to zero, and this time was sufficient in the mini-MSR environment. It is possible that in other environments it will take longer time. After zeroing, the internal calibration numbers are queried from the two QZFMs, shown in Fig. 9. From Quspin's documentations [3], a calibration number below 1.5 indicates very good sensor performance. Here all 6 numbers are below 2, and several below 1.5. Therefore the sensors are performing well.

Finally in Fig. 10 we show in the top graph the compensation field generated by the two sets of coils as a function of time, and in the bottom graph the actual sensor analog output as a function of time, after zeroing has completed. In this view, it is clear that the two sets of PIDs are very successful in reaching

Figure 8: Connection of modulation sharing cable. The cable goes from the Master Mod of the master electronics to the mod in of the first slave.

```
In [25]: AAL9.calibrate()
2024-04-09 09:56:30.778053  Calib X:1.84,Y:0.91,Z:1.52,
(XY)-0.28,(XZ)0.05,(YX)0.56,(YZ)0.02,(ZX)0.04,(ZY)-0.01

In [26]: AAY4.calibrate()
2024-04-09 09:56:43.469120  Calib X:1.90,Y:1.11,Z:2.04, (XY)0.10,
(XZ)0.16,(YX)0.02,(YZ)0.42,(ZX)0.05,(ZY)-0.31
```

Figure 9: Internal calibration numbers reported by the two QZFMs. The calibration numbers for the 3 axes are below 2 for both sensors, which indicates healthy or near-healthy performance.

an equilibrium state (indicated by the flatness of the coil fields) after a short amount of time. The sensor readings in the bottom graph demonstrates they are both functional and respond to the excitation signal from a waveform generator. The differing amplitude is merely due to the different distance to the coil.

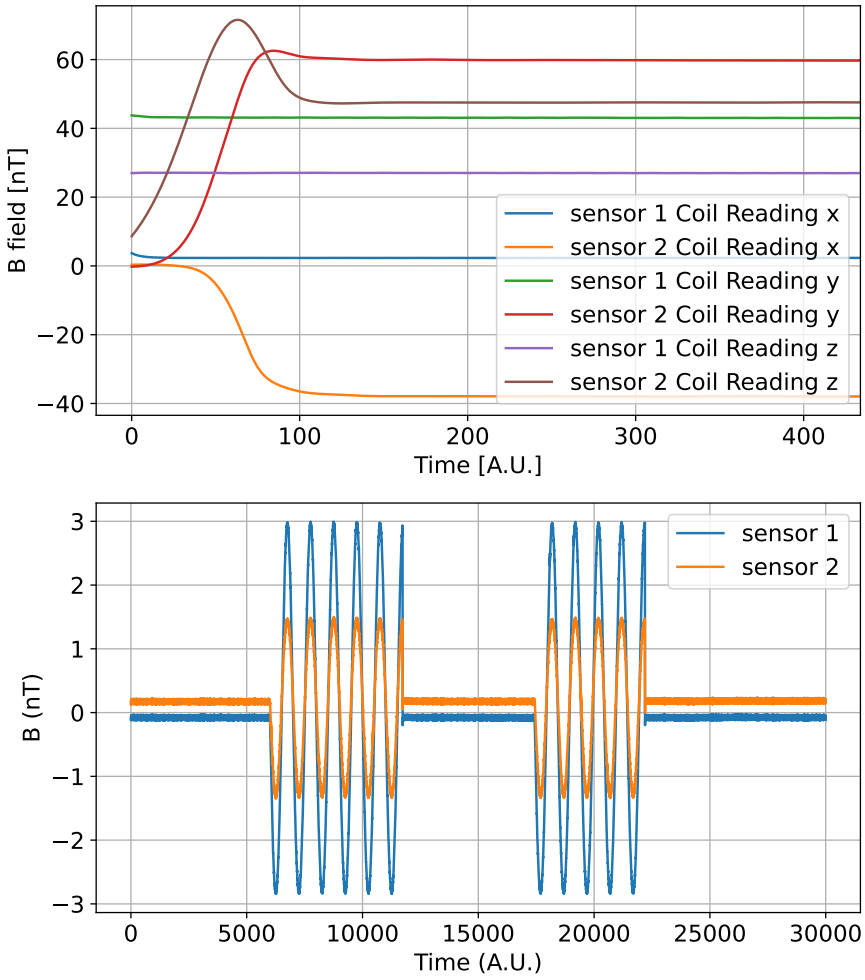

Figure 10: Top: Internal QZFM compensation field as a function of time. All 6 sets of coils successfully reach equilibrium even in the presence of each other. Bottom: Cell reading in the x direction after the two sensors are zeroed. They respond to the same excitation signals and thus are both operational. The different amplitude is due to different displacements from the excitation coil.

References

[1] Elena Boto et al. "Moving magnetoencephalography towards real-world applications with a wearable system". In: *Nature* 555 (7698 2018). ISSN: 14764687. DOI: 10.1038/nature26147.

[2] *Introduction to Zero Field Magnetometer*. URL: https://quspin.com/products-qzfm-gen2-arxiv/zero-field-magnetometer-description/.

[3] *QZFM Quick Start Guide*. URL: https://quspin.com/products-qzfm-gen2-arxiv/qzfm-quick-start-guide/.

[4] Tim M. Tierney et al. *Optically pumped magnetometers: From quantum origins to multi-channel magnetoencephalography*. 2019. DOI: 10.1016/j.neuroimage.2019.05.063.